January 23, 2011

Revealing Time Bunching Effect in Single-Molecule Enzyme Conformational Dynamics

Hong Lu, *Bowling Green State University*

PCCP

Dynamic Article Links

Cite this: *Phys. Chem. Chem. Phys.*, 2011, **13**, 6734–6749

www.rsc.org/pccp

PERSPECTIVE

Revealing time bunching effect in single-molecule enzyme conformational dynamics

H. Peter Lu*

Received 12th December 2010, Accepted 23rd January 2011
DOI: 10.1039/c0cp02860f

In this perspective, we focus our discussion on how the single-molecule spectroscopy and statistical analysis are able to reveal enzyme hidden properties, taking the study of T4 lysozyme as an example. Protein conformational fluctuations and dynamics play a crucial role in biomolecular functions, such as in enzymatic reactions. Single-molecule spectroscopy is a powerful approach to analyze protein conformational dynamics under physiological conditions, providing dynamic perspectives on a molecular-level understanding of protein structure–function mechanisms. Using single-molecule fluorescence spectroscopy, we have probed T4 lysozyme conformational motions under the hydrolysis reaction of a polysaccharide of *E. coli B* cell walls by monitoring the fluorescence resonant energy transfer (FRET) between a donor–acceptor probe pair tethered to T4 lysozyme domains involving open–close hinge-bending motions. Based on the single-molecule spectroscopic results, molecular dynamics simulation, a random walk model analysis, and a novel 2D statistical correlation analysis, we have revealed a time bunching effect in protein conformational motion dynamics that is critical to enzymatic functions. Bunching effect implies that conformational motion times tend to bunch in a finite and narrow time window. We show that convoluted multiple Poisson rate processes give rise to the bunching effect in the enzymatic reaction dynamics. Evidently, the bunching effect is likely common in protein conformational dynamics involving in conformation-gated protein functions. In this perspective, we will also discuss a new approach of 2D regional correlation analysis capable of analyzing fluctuation dynamics of complex multiple correlated and anti-correlated fluctuations under a non-correlated noise background. Using this new method, we are able to map out any defined segments along the fluctuation trajectories and determine whether they are correlated, anti-correlated, or non-correlated; after which, a cross correlation analysis can be applied for each specific segment to obtain a detailed fluctuation dynamics analysis.

Enzymes play a significant role in regulating the biological clocks of living cells; for example, enzymes are capable of changing the biological activity pathways and enhancing a biological reaction rate by as much as 10^{16} times. An enzymatic reaction typically involves active substrate-enzyme complex formation, chemical transformation, and product releasing, as we know of the Michaelis–Menten mechanism. Conformational motions are essential for the catalytic functions of enzymes. Involving in functionally conformational motions, an enzyme adjusts its physical and chemical flexibility towards an active state (ES*), which consists of the binding complex of an enzyme (E) and a substrate (S) for a specific catalytic reaction. Subtle conformational changes play a crucial role in enzyme functions, and these protein conformations are highly dynamic rather than being static. It is the enzyme-substrate interaction and active complex formation that often play a critical role in defining the enzymatic dynamics, energy landscape, and reaction nuclear coordinates and pathways. Using only a static structural characterization, from an ensemble-averaged measurement at equilibrium is often inadequate in predicting dynamic conformations and understanding correlated enzyme functions involving in non-equilibrium, multiple-step, multiple-conformation complex chemical interactions and transformations.

In recent years, one of the most exciting developments in single-molecule spectroscopy is its applications on studying protein dynamics and enzymatic reaction dynamics.[1–18] The static disorder [1,2,19,20] and dynamic disorder[3,19,20] of single-molecule enzymatic reactions have been observed by measuring single-molecule assays,[1,2,21] monitoring co-enzyme redox state turnovers in real-time,[3] and recording enzymatic reaction product formation in real-time.[19,20] Direct observations of conformational changes along enzymatic reaction coordinates are often crucial for understanding inhomogeneities in enzymatic reaction systems.[12] Recently[110], there are a number of excellent

Bowling Green State University, Center for Photochemical Sciences, Department of Chemistry, Bowling Green, OH 43403, USA. E-mail: hplu@bgsu.edu

articles on the broad perspectives of the single-molecule enzymology, and we would like to focus our perspective discussion, from a different angle, on a number of newly developed technical approaches and their applications of identifying and revealing some hidden enzyme conformational dynamics crucial for a fundamental comprehension of the enzymolgy. We will first provide a perspective of current technical approaches on probing single-molecule enzymatic reaction correlated conformational dynamics, discussing not only the advantageous capabilities but also the limitations and possible future improvements. We will then focus our discussion on a specific example of our work on studying single-molecule T4 lysozyme enzymatic dynamics using a number of novel single-molecule experimental approaches and statistical analyses. Finally, we will provide a broader perspective on the future development of the single-molecule conformational dynamics research field.

1. The technical limitations and possible improvements of single-molecule enzymology analyses

Single-molecule enzymology has been under a rapid development. A few different single-molecule assays have been demonstrated by probing: (1) single molecule products,[4,5,105,106] (2) individual electrophoresis zones of products from a single enzyme,[1,2] (3) single substrate molecules,[80] (4) a fluorescent enzyme active site,[3] (5) intermolecular smFRET,[81] and (6) intramolecular smFRET.[12] Each approach has advantages and shortcomings. Probing single molecules of product or substrate directly measures the individual enzymatic reaction turnovers in real time. Probing the zones of product molecules obtains the overall single-molecule enzymatic reaction rates, but provides little or no information on the reaction-associated enzyme conformational changes. Probing fluorescent active-site fluorescence, however, can yield information on both single-molecule enzymatic reaction dynamics and the collective active-site conformational fluctuation dynamics. For example, probing the redox state of a co-enzyme, flavin adenine dinucleotide, toggles between an oxidized and reduced states in cholesterol oxidase enzymatic reaction turnovers.[3] However, such approach makes it difficult to identify and measure the specific activity-regulating conformational changes in an enzymatic reaction. Recently, it has been demonstrated that smFRET is able to obtain detailed characterization and analysis of the conformational change dynamics and energy landscape.[12] On the other hand, the limitation of the smFRET approach is that the enzymatic reaction turnovers can only be assured statistically but not assigned individually, since there is a statistical probability of non-productive conformational motions in the reactive nuclear coordinates. Using a single-molecule fluorescence spectroscopic measurement, it is still extremely hard to probe simultaneously the single-molecule enzymatic reaction turnovers, the product generation or substrate consumption, and the specific conformational changes. There is typically a trade-off in probing one critical parameter. Furthermore, one property of fluorescence molecules that limits the length of time that single-molecule trajectories can be acquired is their ability to undergo photobleaching. We have found that a single molecule can, on average, emit about 1 million photons before the molecule is irreversibly photobleached. With a typical 10 percent photon detection efficiency, we could record sufficiently long single-molecule fluorescence trajectories for sound statistical analysis. Therefore, single-molecule fluorescence trajectories can be acquired for as long as minutes using lower laser excitation photon flux and a longer bin time, or they can be acquired for as short as subseconds using a higher laser excitation photon flux but shorter bin time, leading to a higher time resolution. Nevertheless, enzymatic reactions typically involve an inhomogeneous environment and complex mechanism; it is often crucial to probe directly the specific conformational changes involved in an enzymatic reaction. For example, the hinge-bending motions associated with the T4 lysozyme hydrolysis enzymatic reaction are critical but cannot be studied by either conventional ensemble-averaged measurements or alternative approaches, other than single-molecule intramolecular smFRET.[12] The approaches described in this perspective have the advantage of characterizing the enzyme-activity-related conformational fluctuation without directly probing the product release. A combined approach to probe both parameters is still a great challenge for single-molecule enzymology due to the congestion of the fluorescence of the chromospheres. In recent years, using three FRET probe dyes to measure multiple dimensional conformational dynamics has made progresses,[82–84] and a careful selection of the dye molecules may give a chance to circumvent the fluorescence spectral congestion problem.

Typically, single-molecule spectroscopy studies on enzymatic reactions and associated conformational change dynamics have time resolutions longer than sub-milliseconds. It is not only desirable but also critical to probe the conformational change dynamics at an ultra-fast time-scale, nanoseconds or even picoseconds, because many important protein

H. Peter Lu

H. Peter Lu received his BS and MS in Chemistry from Peking University in 1982 and 1984. He moved to the United States in 1986 after two-year teaching at Peking University, and he received his PhD degree in physical chemistry from Columbia University in 1991. After postdoctoral work at Northwestern University and the Pacific Northwest National Laboratory, he worked at the Pacific Northwest National Laboratory as a senior research scientist and later as a chief scientist from 1996 to 2006. He moved to Bowling Green State University in Ohio as a Ohio Eminent Scholar and professor of chemistry in 2006. Focusing on condensed phase chemical physics and dynamics, his primary research interests are in single-molecule spectroscopy and microscopy, single-molecule protein conformational dynamics, and interfacial chemical and biophysical dynamics.

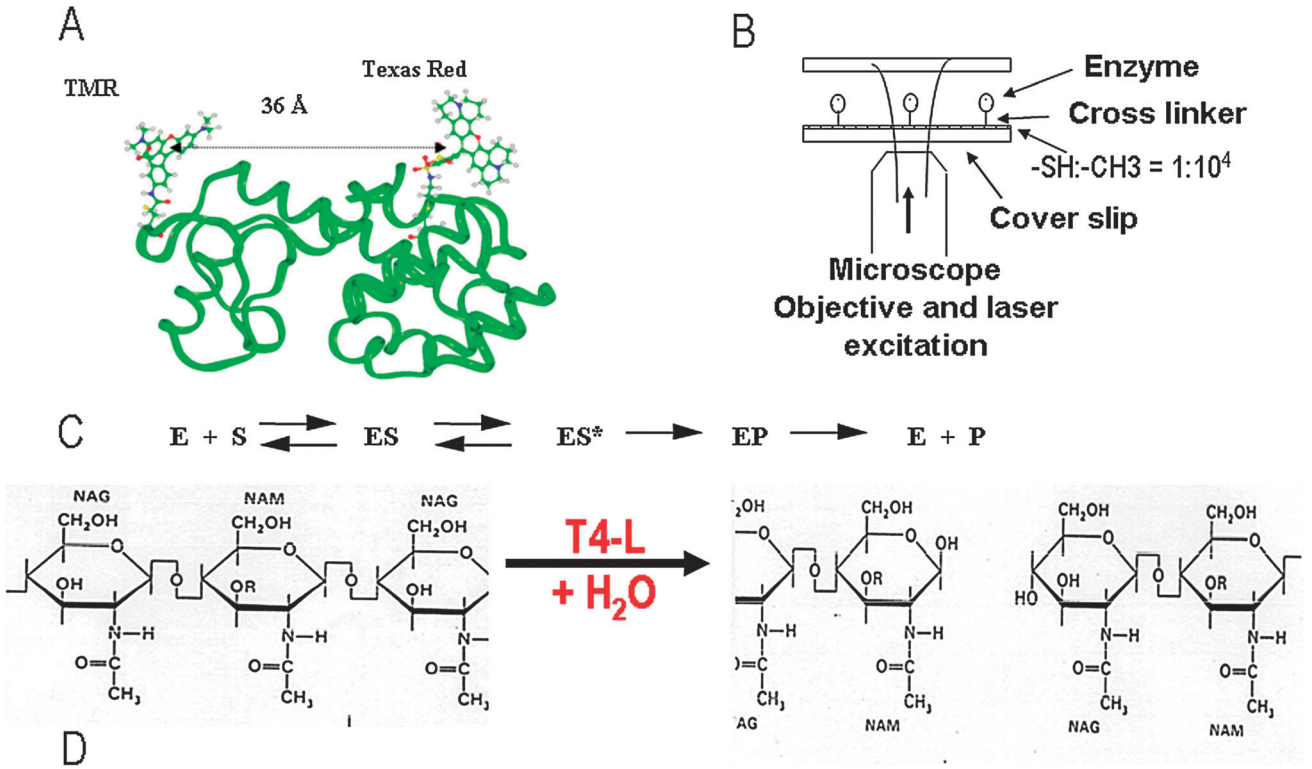

Fig. 1 Probing single-molecule T4 lysozyme conformational dynamics in enzymatic hydrolysis of polymer sugar chain substrates. (A) Crystal structure of wild-type T4 lysozyme. The protein was labeled with Texas Red maleimide and tetramethylrhodamine iodoacetamide (or Alexa 488/Alexa 594 dye probes) by thiolation to Cys-54 and Cys-97. The significant advantage of our site-specific covalent dye labeling is that the attached donor–acceptor pair can sense the relative motion of the two domains in T4 lysozyme without perturbation of the enzymatic activity.[12] (B) The T4 lysozyme was covalently linked to a hydrocarbon-modified glass cover slip by the bi-functional linker SIAXX (Molecular Probes, Inc.). At 10^{-9} M concentration, the single-molecule enzyme molecules on surface in a density less than 1 molecule per mm^2 so that the diffraction-limited laser spatial focused spot can conduct single-molecule FRET excitation and measurement at an individual molecule at a time. (C) A typical Machelis-Menton mechanism involving that enzyme (E) forming non-specific binding complex (ES) with the substrate (S), and then transform to active complex (ES*) mostly though conformational changes, and then chemical reaction (EP) followed by product releasing (E + P). (D) Hydrolysis reaction of polyssacharide.

conformational motions are at nanosecond time-scale.[34,35] Moreover, inhomogeneous protein conformational dynamics often show a power-law behavior extended in a wide time range from seconds to nanoseconds. Our group[41] and others[85,86] have developed photon-stamping single-molecule fluorescence detection techniques that can measure single-molecule ultra-fast fluorescence anisotropy dynamics.[41,86] The single-molecule nanosecond anisotropy is readily applicable to probing protein conformational dynamics by tethering bi-functional dyes[87,88] or tetradentately-attached dyes[41,89–91] to specific sites or domains of the proteins. For example, a mutant T4 lysozyme can be used with two cysteine residues at the same distance as the bi-functional dye can be labeled. A bi-functional fluorescent probe can be used to anchor it on the protein surface across two cysteine residues so that the dye molecule self-wobbling motions are fixed and only the protein matrix motion is probed. Therefore, the inter-domain and intra-domain conformational dynamics of a protein can be studied by probing the fluorescent dipole rotational motion without the complication of convoluted dye motions. Noticeably, the nanosecond single-molecule dynamics studied by single-molecule nanosecond anisotropy can be directly comparable and correlated with single-molecule dynamics from a molecular dynamics simulation.

2. Probing the single-molecule hinged-bending motions of T4 lysozyme in catalytic reactions

We have applied single-molecule spectroscopy and imaging to studying complex enzymatic reaction dynamics and the enzyme conformational changes, focusing on the T4 lysozyme enzymatic hydrolyzation of the polysaccharide walls of *Escherichia coli B* cells. The lysozymes destroy bacterial cell walls by hydrolyzing the polysaccharide component of the peptidoglycan matrix (Fig. 1). Using this system provides us with a way to gain a fundamental understanding of how nano-scale structures control the complex chemical reactions in condensed phase. Wild-type lysozyme has two domains connected by an α-helix (Fig. 1A).[22–25] The structure and enzymatic activity of wild-type lysozyme and its mutants have been investigated extensively by X-ray crystallography,[22–25] NMR,[26,27] site-directed spin labeling,[28] and molecular dynamics simulations.[29] The enzyme consists of two domains adopting different conformations of the active site cleft, including open and closed states[22–27] involving in hinge-bending motions in forming enzyme-substrate complex (Fig. 1B).[23–27,30] By attaching a donor–acceptor pair of dye molecules site-specifically to non-interfering sites on the enzyme, we were able to measure

the real-time hinge-bending conformational motions of the active enzyme by monitoring the donor–acceptor emission intensity as a function of time. We have also explored a combined approach, applying molecular dynamics (MD) simulation, a random-walk model analysis, and a novel 2D correlation amplitude mapping analysis based on the single-molecule experimental data. This combination of experimental and theoretical methodology represents a new approach to obtaining conformational coordinate-specific enzymatic reaction dynamics. Using this approach, we analyzed enzyme-substrate complex formation dynamics to reveal (1) multiple intermediate conformational states, (2) oscillatory conformational motions, and (3) a conformational time bunching effect in the chemical reaction process.[13]

3. The bunching effect in T4 lysozyme enzymatic conformational dynamics

The bunching effect observed in T4 lysozyme enzymatic conformational dynamics is novel, and it is distinctively different from the previously reported memory effect in enzymatic reaction dynamics. A memory effect, an enzymatic reaction turnover time dependent on its previous turnover time, has been extensively reported in recent years.[3,4,44,52–54] The typical characteristics of a memory effect in dynamics is that a long turnover time is likely to be followed by a long one, and a short turnover time is likely to be followed by a short one in enzymatic reaction. The quantitatively description of the memory effect is by using autocorrelation function of a single-molecule turnover time trajectory and the diagonal features in a two dimensional joint probability distributions. Based on a number of recently published experimental results and simulations, slow functional conformational motion and equilibrium conformational fluctuations in enzymatic turnovers have been suggested to be responsible for memory effects in the enzymatic turnover cycles, such as for cholesterol oxidase.[3,9,44] The bunching effect for enzymatic conformational dynamics reported here is related but significantly different from the previously reported memory effect. For a typical memory effect in enzyme conformational motions under an enzymatic reaction, the conformational motion times may cover a broad time scale of many folds along the diagonal direction in a two dimensional joint probability distributions, and second moment of the time distribution is not necessarily finite as the time distribution is non-Gaussian and often Lévy or Lorenzin.[48–50] However, in a bunching effect associated conformational dynamics presented later in this perspective and recent publication,[12] the conformational motion times distribute in a relative narrow range and the data points show bunching at a specific area along the diagonal direction in a two dimensional joint probability distribution plot. The second moment of the time distribution is finite and the time distribution is Gaussian or Gaussian-like. Furthermore, for the dynamics showing memory effect, the 2D joint probability distribution, $f(t_i, t_{i+j})$, changing with the time separation index j: as j increases the diagonal feature intensity decreases as the memory only exist for a finite time; whereas for the bunching effect, the 2D joint probability distribution is essentially stationary with changing j, and the bunching effect demonstrates a stable impact on the enzyme function and dynamics as long as the external environment and reaction condition are kept the same. Bunching effect often shows a strong regulation and controlling impact in conformation-gated protein function and dynamics. We suggest that bunching effect and memory effect, both as typical dynamic behaviors of non-equilibrium enzymatic reaction dynamics, are two general behaviors that commonly occur in the enzymatic conformational dynamics, especially for conformational regulated enzymatic reactions. Their occurrence possibilities are determined by the nature of the conformational motions, which is regulated by the interaction between enzyme and substrate, such as geometrical constraints, solvent perturbation, electrostatic interaction, hydrophobicity, and binding modes.

4. Single-molecule fluorescence resonant energy transfer spectroscopy probing enzymatic conformational dynamics

In our single-molecule fluorescence resonant energy transfer (smFRET) experiments, appropriate fluorescent probes were covalently attached to the Cys residues of the proteins. By controlled reaction conditions and carefully chosen dye derivatives with appropriate functional linking groups, we were able to get high yield, purified single-dye or double-dye (donor–acceptor) labeled proteins. For example, we site-specifically labeled two cysteines with tetramethylrhodamine (TMR iodoacetamide) and Texas Red (Texas Red maleimide) on wild-type Lysozyme protein through thiolation, and conducted FRET studies of single-molecule Lysozyme enzymatic reactions and coordination-specific conformational changes (Fig. 1A). The effects of fluorescence labels on enzyme proteins were typically evaluated by comparing enzymatic assays for native protein and labeled proteins. We have found that dye labeling can cause a wide range of perturbations to the enzyme activity: from no effect (for example, wild-type lysozyme) to up to more than 30% (for example, mutant (E11A) lysozyme) predominately depending on the sites of the dye labeling.

Our single-molecule spectroscopy approach has shed light on a number of fundamental questions about the conformational dynamics related to the enzymatic reaction mechanism: For example, what are the spatial and temporal ranges of the critical nanoscale conformational motions occurring during chemical processing by lysozyme? Can we obtain coordinate-specific characterization of these dynamic motions? Can the inter-domain and intra-domain conformational motions be characterized and differentiated in the context of the overall reaction mechanism and dynamics? Do complexes formed between the enzyme and its substrate associate, dissociate and change conformations at inhomogeneous rates? Can the origin of the inhomogeneity be characterized? How sensitive are the distributions of the rates to local environmental conditions? Typically, these critical questions are extremely difficult to be analyzed by conventional ensemble-averaged approaches. Nevertheless, there is an unprecedented opportunity to gain significant progress on tackle these questions by single-molecule spectroscopy approaches.

The real-time point-to-point distance change measurements using smFRET have provided a direct visualization of the molecular motions throughout the course of the searching, binding, activation, reaction and product release steps the enzymatic reaction events. We note that smFRET can reliably measure the distance fluctuation dynamics but not necessarily the absolute distance. By using single-molecule spectroscopic approaches, we were able to characterize the spatial distributions of substrate-protein distance changes and the temporal fluctuations of these structures throughout the reaction pathway; the temporal ranges include protein motion and conformational change dynamics from sub-seconds to microseconds. The most critical protein motions often involve substantial rearrangements and can cover a wide time range (millisecond to seconds). Nanoscale conformational motions often have intrinsically disordered regions that exhibit large conformational changes during the reaction process which are critical to enabling the reaction. We have tested whether relatively slow (sub-millisecond to second) protein motions are the most critical in the reactions or whether fast motions are the key and identify the static and dynamic distributions of the protein motion rates. The protein rotational motion and local electric field fluctuation dynamics can be studied by the fluorescence anisotropy from intrinsic fluorophores or a dye with high sensitivity to the local electric field.

Static disorder and dynamic disorder in the ensemble of interactions result in inhomogeneous rates in ways that are sensitive to changes in environmental conditions and that can vary highly from molecule to molecule. Presumably, substrate-protein complexes dissociate and change conformations at inhomogeneous rates, their static and dynamic distributions, and the environmental conditions (local protein concentrations, pH, ionic strength, temperature, viscosity, *etc.*) can all affect the distributions.[12] Single enzyme-substrate complexes can be visualized through monitoring single-molecule time trajectories of binding motions under different local environments in combination with statistical model analyses[3,10,31,32] and computational simulations.[8] Molecular-level understanding of the effects of the local nano-environment is crucial for understanding and modeling the complex enzymatic reactions in cell wall hydrolysis that are present in a wide range of temporal and spatial environments.

5. T4 lysozyme conformational changes under enzymatic reaction turnovers

The domain motion of T4 lysozyme is rather complex and contains motions besides hinge-bending. It is reasonable to assume that the hinge-bending motion in nature involves multiple coupled nuclear coordinates that can be projected to a nuclear coordinate associated with the α-helix. Based on our study[12] and a previous[18] molecular dynamics simulation of wild-type T4 lysozyme in solution, the distance change between the two dye-tethered cysteine residues is from 30.5 Å to 35 Å, *i.e.*, the donor–acceptor distance change is about 4.5 Å. We estimated the Förster distance R_0[19] of a TMR/Texas Red pair to be about 50 ± 5 Å. The lengths of the two covalent linking groups of the donor and acceptor dipoles, which have an actual donor–acceptor distance change of 5.5 Å,[12] can cause a change of 2–3 times in donor fluorescence intensity.[12,19]

To demonstrate the feasibility of applying FRET to probe the conformational changes of T4 lysozyme proteins under binding and unbinding hinge-bending motions, we measured the ensemble-averaged FRET emission spectra from the donor–acceptor-labeled T4 lysozyme, both with and without the substrates (Fig. 2). The ratio of spectral intensities of the donor emission *vs.* acceptor emission significantly increases on attaching to the substrate. The ensemble fluorescence intensity measurement indicates the conformation change of T4 lysozyme upon binding to the substrate although it is essentially a qualitative confirmation of FRET existence under the interaction between the enzyme and substrate.

The fluorescence intensity trajectories of the donor ($I_d(t)$) and acceptor ($I_a(t)$) give autocorrelation times (Fig. 3) indistinguishable from fitting an exponential decay to the autocorrelation functions, $\langle \Delta I_d(0)\Delta I_d(t)\rangle$ and $\langle \Delta I_a(0)\Delta I_a(t)\rangle$, where $\Delta I_d(t)$ is $I_d(t) - \langle I_d\rangle$, $\langle I_d\rangle$ is the mean intensity of the overall trajectory of a donor, and $\Delta I_a(t)$ has the same definition for an intensity trajectory of an acceptor. In contrast, the cross-correlation function between the donor and acceptor trajectories, $\langle \Delta I_d(0)\Delta I_a(t)\rangle$, is anticorrelated with the same decay time (Fig. 3C), which supports our assignment of anticorrelated fluctuations of the fluorescence intensities of the donor and acceptor to the smFRET process. Our further control experiment of nanosecond anisotropy proved that the tethered enzyme can freely rotate and has a minimum perturbation from the hydrocarbon-modified glass surface (Fig. 4).[12] We used femtosecond laser pulse excitation in the single-molecule anisotropy measurements, and we were able to probe the nanosecond molecular rotational motions when the single T4 lysozyme enzyme molecules were confined in the agarose gel, suggesting the enzyme molecules are confined but free in rotational motions.

Single-molecule smFRET fluorescence trajectories contain detailed information about the conformational motion associated with the enzymatic turnovers. The upper panel in Fig. 5 shows an expanded portion of a trajectory (middle panel) recorded from donor fluorescence of a single-pair donor–acceptor labeled protein with substrate present. By comparison, the lower panel shows a portion of a donor-fluorescence trajectory recorded from a donor-only labeled T4 lysozyme under the same conditions. The large-amplitude, lower-frequency wiggling of the donor fluorescence intensity in the upper panel is largely absent from the trajectory in the lower panel. The inset in Fig. 5 (middle panel) shows a bimodal fluorescence intensity distribution that reflects the open and closed conformational states of a T4 lysozyme. By contrast, only a Poisson-shaped distribution was deduced from the trajectory of a donor-alone labeled single enzyme molecule. This indicates that only fast fluctuations and uncorrelated noise were recorded, since the donor dye alone is not sensitive to the enzyme open-close hinge-bending motions (Fig. 5, lower panel).

We have attributed each wiggle to a hinge-bending motion involved in either an enzymatic reaction or nonproductive binding and releasing of the substrate.[12] The donor fluorescence intensity increases as the active site opens due to substrate inserting and decreases as the active site closes to form an active enzyme-substrate complex. This attribution is consistent with the systematic control results of the ensemble-averaged

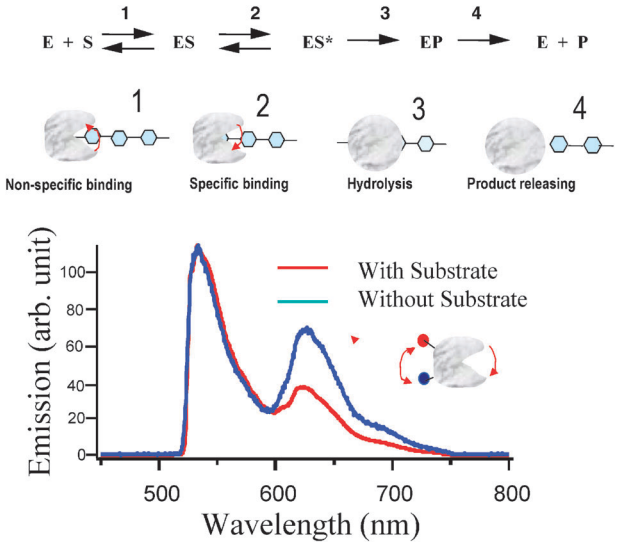

Fig. 2 Ensemble-averaged control FRET essay of probing T4 lysozyme conformational open-close motions, opening up to intake the substrate and binding down to form the active complex (ES*), in hydrolysis of an *E. coli B* cell wall. There are no significant conformational changes in reaction and product releasing; therefore, for each enzymatic reaction cycle, there is an open-close enzymatic conformational motion involved. The fluorescence spectra of Alexa 488/Alexa 594 labeled T4 lysozyme mutant (E11A) excited at 488 nm. The blue and red lines are the fluorescence spectra of the enzyme in solution without and with substrate *E. coli B* cell walls present, respectively. The two spectra are normalized to the same maximum point, to aid the view. It is clearly shown that the FRET efficiency significantly decreased when the enzyme is under enzymatic reaction with the substrates. The decrease of the FRET efficiency is due to the two domain of the enzyme involve in open-close conformational motions spending more time averagely in the conformations that the two domains are farther away in open state. We note the enzymatic reaction equation in this figure only presents a conceptual interpretation of the catalytic mechanism. Our later discussion will specify a detailed characterization of the mechanism.

FRET measurements and the single-molecule FRET intensity fluctuation dynamics analysis made with and without a substrate.[12] Further evidence that we are measuring the hinge-bending motion comes from evaluating autocorrelation functions calculated from the single-molecule donor and acceptor trajectories when changing the laser excitation intensity, the pH, and the substrate concentration.[12] We did not observe a dependence of fluctuation correlation time on the excitation rate, indicating that the fluctuations were spontaneous rather than laser-driven. However, we did observe autocorrelation rate constants that differed by a factor of 2 over the pH range from 7.2 to 6.0.[12] This two-fold decrease in decay rate constant is consistent with the enzymatic activity decrease measured by ensemble-averaged assays at pH 7.2 and 6.0.[34]

6. Mechanistic understanding of the conformational dynamics in T4 lysozyme enzymatic reaction

Based on our single-molecule experimental trajectory data (Fig. 5), the donor–acceptor distance and the donor fluorescence intensity increase when the active site opens up to form a nonspecific binding complex (ES) with the substrate, corresponding to the process of E + S → ES. The donor–acceptor distance and the donor fluorescence intensity decrease when the active site closes to form an active complex (ES*), corresponding to the process of ES → ES* (Fig. 1B, 2, 5 and 6). There are no measurable smFRET changes, implying no significant conformational motions in the process ES* → EP or in the product-releasing process of EP → E + P (Fig. 2 and 6).

The formation of ES and ES* involves significant domain breathing-type hinge-bending motions along the α-helix (Fig. 6) and is probed in real time by recording single-molecule smFRET trajectories that record the formation times, t_{open}, of enzymatic intermediate ES and ES* states from the single-molecule enzymatic turnover trajectories (Fig. 5).[12] Fig. 7A shows a Gaussian-shaped distribution of the open-time (t_{open}) deduced from a single-molecule trajectory. The first moment of the distribution, $\langle t_{open} \rangle = 19.5 \pm 2$ ms, corresponds to the mean time of the processes of E + S → ES → ES*, as shown in Fig. 7B and C. The standard deviation of the distribution, $\sqrt{\langle \Delta t_{open}^2 \rangle} = 8.3 \pm 2$ ms, reflects the distribution bandwidth. For the individual T4 lysozyme molecules examined under the same enzymatic reaction conditions, we found that the first and second moments of the single-molecule t_{open} distributions are homogeneous, within the error bars. The hinge-bending motion allows sufficient structural flexibility for the enzyme to optimize its domain conformation: the donor fluorescence essentially reaches the same intensity in each turnover, reflecting the domain conformation reoccurrence. The non-equilibrium conformational motions in forming the active enzymatic reaction intermediate states intrinsically define a recurrence of the essentially similar potential surface for the enzymatic reaction to occur, which represents a time bunching effect in the enzymatic reaction conformational dynamics.[12,35,36,42]

The Gaussian-like distribution of the t_{open} and the ramping changes of intensity at a millisecond time-scale in the single-molecule fluorescence time trajectories suggest that the protein hinge-bending conformational changes involve multiple intermediate conformational states and time bunching effect.[3–5,12,35,42] The bunching effect is intrinsic due to that the dominant nuclear coordinate is essentially the same for the bending motion that opens and closes the active site and, most likely, is associated with the α-helix hinge of the T4 lysozyme and relatively identical substrate-enzyme electrostatic force of the induced conformational changes. It is likely that the substrate binding selectively shifted the equilibrium among the fluctuating conformations of the enzyme which energetically and dynamically regulated the hinge-bending motions into a specific conformational fluctuation time range. The results of the MD simulation[12] suggest that the dominant driving force for E + S → ES is the positive surface charge of the enzyme from surface amino acid residues (arginine and lysine) interacting with the negatively charged polysaccharide substrate. The driving force for ES → ES* includes the formation of six hydrogen bonds in the active site of ES*.

We model the hinge-bending motion associated with interactions between the enzyme and substrate as a classical particle one-dimensional multiple-step random walk in the

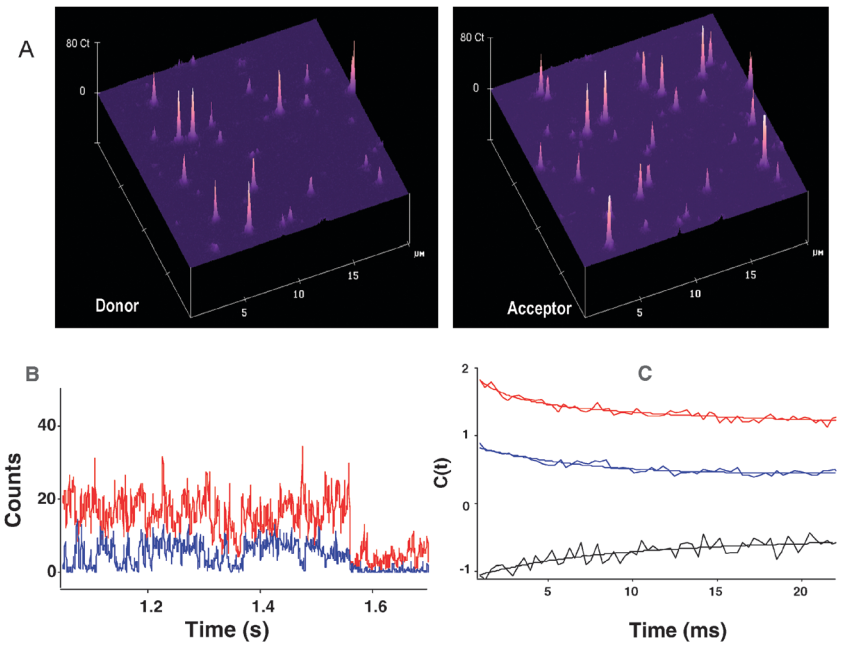

Fig. 3 Single-molecule recording of T4 lysozyme conformational motions and enzymatic reaction turnovers of hydrolysis of an *E. coli B* cell wall in real time. (A) Fluorescence image (20 mm × 20 mm) of single-T4 lysozyme molecules tethered to the hydrocarbon-modified glass surface of a cover slip under pH 7.2 buffer aqueous solution. The fluorescence emission was split by a dichroic beamsplitter (595-nm long-pass). The donor (**left panel**) and acceptor (**right panel**) emissions were detected separately by a pair of avalanche photodiode detectors after passing through a 570-nm band-pass filter (20-nm bandwidth) and a 615 nm long-pass filter, respectively. The two images were taken from the same area of a sample with an inverted fluorescence microscope by raster-scanning the sample with a focused laser beam of 100 nW at 532 nm. Each individual peak is attributed to a single T4 lysozyme molecule. The intensity variation among the molecules is predominately due to smFRET. (B) This panel shows a pair of trajectories from a fluorescence donor tetramethylrhodamine (blue) and acceptor Texas Red (red) pair in a single-T4 lysozyme in the presence of *E. coli* cells of 2.5 mg mL^{-1} at pH 7.2 buffer. Anticorrelated fluctuation features are evident. (C) The correlation functions (C(t)) of donor ($\langle \Delta I_d(0)\Delta I_d(t)\rangle$, blue), acceptor ($\langle \Delta I_a(0)\Delta I_a(t)\rangle$, red), and donor–acceptor cross-correlation function ($\langle \Delta I_d(0)\Delta I_a(t)\rangle$, black), deduced from the single-molecule trajectories in (A). They are fitted with the same decay rate constant of 180 ± 40 s^{-1}. A long decay component of 10 ± 2 s^{-1} is also evident in each autocorrelation function. The first data point (not shown) of each correlation function contains the contribution from the measurement noise and fluctuations faster than the time resolution. The correlation functions are normalized, and the $\langle \Delta I_a(0)\Delta I_a(t)\rangle$ is presented with a shift on the **y** axis to enhance the view.[12]

presence of a force field.[12,37] From this model analysis, we have deduced an analytical solution showing

$$D = \frac{\left(\sqrt{\left\langle \Delta t_{open}^2 \right\rangle}\langle X_N(t)\rangle\right)^2}{2\langle t_{open}\rangle^3} \qquad (1)$$

where D is the diffusion coefficient.

The total drifting distance of the conformational open-close motion in one enzymatic reaction turnover, $\langle X_N(t)\rangle$, is about 9 Å, based on our smFRET measurements and MD simulation.[12] The mean open-time, $\langle t_{open}\rangle$ and the standard deviation of the open-time distribution, $\sqrt{\langle \Delta t_{open}^2\rangle}$, were measured to be 19.5 ± 2 ms and 8.3 ± 2 ms, respectively. Therefore, the mean drifting velocity, $\langle v\rangle = \langle X_N(t)\rangle/\langle t_{open}\rangle$, of the conformational change in E + S → ES → ES* is $\langle v\rangle = 4.6 \times 10^{-6}$ cm s^{-1}, and the diffusion coefficient is, therefore, $D = 3.8 \times 10^{-14}$ cm^2/s.[12,35]

We further characterized the energy landscape of the hinge-bending conformational change dynamics by estimating that the minimum number of conformations is $m = \langle X_N(t)\rangle/L = 5.6$, where L is the single step size of the random walk diffusion. The average rate for each step is $m/\langle t_{open}\rangle = 280$ s^{-1}. This result of $m > 2$ at the limit of $k_b \to 0$ suggests that there are more than two conformational intermediate states in addition to ES and ES*. With the assumption of $k_b \to 0$, the friction coefficient can be estimated using the Einstein relationship, $\xi = kT/D$, giving $\xi = 1.1$ erg s cm^{-12}. From MD simulation of the E state and the ES* state energies, our best estimate of the total energy change between the two states is −18 kcal mol^{-1} (-1.25×10^{-19} J per molecule) that constitutes the energy gains from electrostatic, van der Waals, and hydrogen-bond formation terms. Therefore, we estimate that 36% of the total energy change between E and ES* is spent on the friction along the reaction coordinate. Since the total energy change between the E state and the ES* state is about −18 kcal mol^{-1}, assuming six intermediate states would result in an average energy difference of 3 kcal mol^{-1} for each associated conformational state along the α-helix coordinate during the hinge-bending motion. We postulate that the activation energy associated with the k_f of the forward step is about 0–5 kcal mol^{-1}, considering the slow forward rate and the entropy decrease in the complex formation process.[14] It is reasonable to assume the energy potential surface along the conformational change nuclear coordinate to be parabolic for each intermediate state. Therefore, the averaged force constant of the potential surface for each intermediate state is calculated to be 3.4–0 kcal mol^{-1} $Å^{-1}$ (Fig. 8).[12,35]

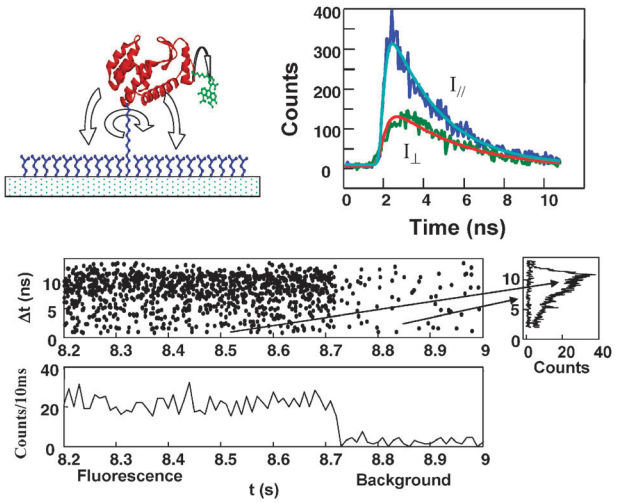

Fig. 4 Single-molecule control experiment to demonstrate that the tethered enzyme is fully mobile in solution by two-channel single-molecule photon time-stamping fluorescence anisotropy spectroscopy. It allows us to study the fluorescence intensity, lifetime, and anisotropy of a single molecule simultaneously by recording the arrival time and delay time of each fluorescence photon. (A) A cartoon shows that the T4lysozyme protein tethered to hydrocarbon modified glass surface through bi-function linker. The enzyme can freely move in buffer solution and its enzymatic activity is not perturbed by the surface. (B) Bottom plot is an example of the raw data of the single-molecule photon time-stamping spectroscopy of a detector channel. Each dot corresponds to a photon detected plotted by its arrival time (t) and delay time (Dt) (raw output from TAC in reverse timing). The fluorescence intensity trajectory (bottom panel) can be calculated from the histogram of arrival time (t) with a given time-bin resolution. The molecule was photo-bleached at 8.71 s. The nanosecond fluorescence decay curves (right panel) are the histograms of the delay time of the fluorescence photons ($t < 8.71$ s) and background photons ($t > 8.71$ s). (C) The parallel and perpendicular fluorescence decay and single exponential fits of a single T4 lysozyme/Alexa 488 molecule covalently linked to surface. The decay curves are integrated from all detected photons of parallel and perpendicular channels before photobleaching.[41]

The single-molecule FRET donor–acceptor fluorescence intensity trajectories can also be analyzed by using a Generalized Langevian Equation (GLE) approach.[38,39] In this approach, the FRET efficiency time trajectories are converted to donor–acceptor distance time trajectories and fluctuation velocity trajectories. A memory kernel and time dependent friction, $\zeta(t)$, can then be deduced from analyzing the autocorrelation function of the velocity time trajectories and convolution fitting using the GLE analysis.[38,39] Based on the fluctuation-dissipation Theorem, the environmental force fluctuation autocorrelation function is defined by the time dependent friction, $k_B T\zeta(t) = \langle F(0)F(t)\rangle$, where k_B is the Boltzman constant, T is the temperature, and $F(t)$ is the fluctuating force.[38–40] Analyzing the force fluctuation dynamics, we observed a slow force fluctuation at the rate of comparable to the hinge-bending open-close conformational motion rate. The force fluctuation around the enzymatic reaction conformational coordinate is not completely random, and it is most likely that the other domains of the enzyme also involve in the conformational fluctuation at a similar rate of hinge-bending motions and the overall fluctuations are coupled to the enzymatic hinge-bending motion dynamics.

7. Bunching effect in single-molecule T4 Lysozyme non-equilibrium conformational dynamics under enzymatic reactions

Bunching effect, implying that conformational motion times tend to bunch in a finite and narrow time window, is observed and identified to be associated with substrate–enzyme complex formation in T4 lysozyme conformational dynamics under enzymatic reactions.[42] We have identified the bunching effect of the substrate-enzyme active complex formation time in T4 lysozyme enzymatic reactions. We have identified that the bunching effect, a dynamic behavior observed for the catalytic hinge-bending conformational motions of T4 lysozyme, is a convoluted outcome of multiple consecutive Poisson rate processes that are defined by protein functional motions under substrate–enzyme interactions; *i.e.*, convoluted multiple Poisson rate processes give rise to the bunching effect in the enzymatic reaction dynamics.[42] We suggest that the bunching effect is likely common in protein conformational dynamics involving in conformation-gated protein functions.[42]

It has been extensively reported that the enzyme may experience a set of intermediate states or transient states before reaching a reactive enzyme-substrate complex state.[5,12,17,43–51] In a complex rate processes, such as a non-equilibrium protein reaction process, with the local environmental fluctuation, non-exponential dynamics can be observed in reaction dynamics and conformational dynamics.[6,52]

We have simulated the T4 lysozyme enzyme-substrate active-state formation time, t_{open} probability distributions measured in our smFRET experiments for the T4 lysozyme enzymatic reaction. We proposed a modified Mechaelis–Menton mechanism of the enzymatic reaction (Fig. 9) based on the experimental data and the Random Walk model analysis discussed above. The probability function $P_{(Tn)}$ (for six intermediate steps, $n = 1, 2, 3, 4, 5, 6$) of the formation times was then obtained from the convolution model and the simulation.

Here, in Fig. 9, ES_1 represents a non-specifically bound complex state and ES* represents a specifically bound complex ready to react. The enzymatic reaction is primarily driven by the electrostatic attraction between the positively charged surface of T4 lysozyme's surface amino acid residues (arginine and lysine) and the negatively charged polysaccharide substrate. Being propelled by the electrostatic attraction, the positively-charged front surface of the T4 lysozyme and the negatively-charged substrate approaches to each other to form an enzyme-substrate non-specifically bounded complex states, ES_n. During the enzyme-substrate interaction, six hydrogen bonds[12,17] form at the enzyme active site with the substrate to form the active complex, ES*. Considering the perturbation of the local environment and thermal effect, the step between any adjacent states (for example, from state ES_{n-1} to state ES_n or from the last intermediate state to the active state ES*) is a stochastic process, and the step time obeys Poisson statistics showing a single exponential distribution as

$$P(t) = A[\exp(-t/\tau)] \quad (2)$$

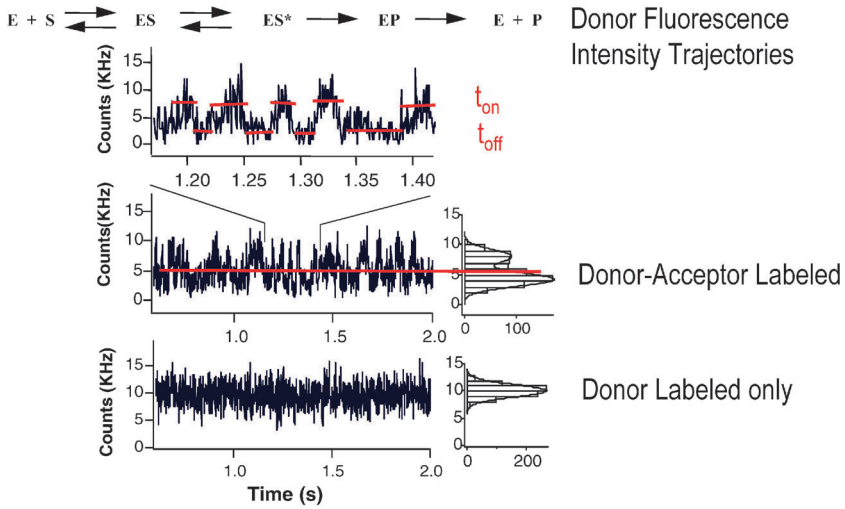

Fig. 5 Real-time observation of single-lysozyme conformational motions and enzymatic reaction turnovers during hydrolysis of bacterial cell walls. The data in the three panels were recorded at 0.65 ms per channel for the same reaction conditions. The upper panel shows an extended portion of middle-panel trajectory of the donor fluorescence of a donor–acceptor labeled single-lysozyme. Intensity wiggles in the trajectory are evident. The lower panel shows a portion of a trajectory recorded from a donor-only-labeled protein. The fluorescence intensity distributions derived from the two trajectories are shown in the insets of the middle and lower panels. The solid lines are fits using single and bimodal Gaussian functions, respectively. The formation of ES and ES* involves significant domain breathing motions along the a-helix "hinge" causing the large amplitude wiggles and the bimodal amplitude distribution. From this it can be seen that smFRET measurements are effective real-time probes of the enzymatic reaction dynamics.[12]

where $P(t)$ is the probability distribution of the step times, τ is the averaged step time, and A is the distribution weight constant. Based on our experimental data, the average formation time of the T4 lysozyme enzymatic reaction in forming the active complex ES* is 19.5 ms (Fig. 7), and the enzymatic reaction experienced about six intermediate steps during the formation time.[16] Since the conformational motions probed are primarily along the hinge-bending motion coordinate and driven by electric static interaction of enzyme–substrate interaction for forming six hydrogen bonds, it is reasonable to assume that the sub-steps in forming the ES* are Poisson processes with the similar rates, and the time distribution for each sub-step obeys eqn (2). For the convoluted intermediate state transition, one can get the probability function $P_{(Tn)}$ from the integral algorithm of eqn (3). To calculate the convolution of function $f(t)$ and $g(t)$, the particular integral transform is:

$$(f * g)(t) = \int_0^t f(\upsilon) \cdot g(t-\upsilon)\mathrm{d}\upsilon \qquad (3)$$

We then have $P_{(T6)} = A^6\{t^5[\exp(-t/3.25)]\}/120$. The general probability function is deduced to be:

$$P_{(Tn)} = A^n \frac{t^{n-1}[\exp(-t/\tau)]}{(n-1)!} \qquad (4)$$

Where n (1, 2, 3...N) is the index of the intermediate steps; τ is the mean step time of an intermediate state through a single-step rate process. The probability functions of the convoluted multiple intermediate states (or transient states) presented here can also be applied to other single-molecule enzyme conformational dynamics.

Based on the function $P_{(Tn)}$ (n = 1, 2, 3...6) of eqn (4), the distribution of conformational motion time for multiple consecutive intermediate steps in forming the active complex of ES* is simulated. The histogram of the simulated formation times for only one intermediate step shows a typical Poisson distribution (Fig. 10A1) and a characteristic wing feature in the 2D joint probability distribution (Fig. 10A2), implying that there is no correlation and bunching effect in the formation times. This is consistent with the stochastic nature of the Poisson rate process. However, the histograms of simulated conformational motion times involved in multiple intermediate steps shown non-Poisson distribution and even Gaussian-like distributions (Fig. 10B1–D1). The simulated conformational motion times involving multiple intermediate states unambiguously show bunching effect as evident by the 2D joint probability distributions (Fig. 10B2–D2). The observed bunching effect implies that the conformational motion time tends to be distributed in a finite and narrow time window as a Gaussian-like distribution with defined and comparable first and second moments.

The existence of the bunching effect in the conformational motion time has significant implications: the hinge-bending open–close conformational motions optimize the physical and chemical flexibilities of the enzyme to similar domain configurations for forming the same ES* complex in the enzymatic reaction turnover cycles. The physical picture suggests strongly that the conformational dynamics of T4 lysozyme shows a characteristic behavior of enzyme conformation selection dynamics driven by substrate-enzyme interactions. In a Poisson rate process, there should be no bunching among the stochastic conformational motion times. However, a non-equilibrium rate process through a sequence of consecutive Poisson processes with comparable rates, eventually produces a bunching effect within the overall time lapse for the overall multiple-step rate process (Fig. 10).

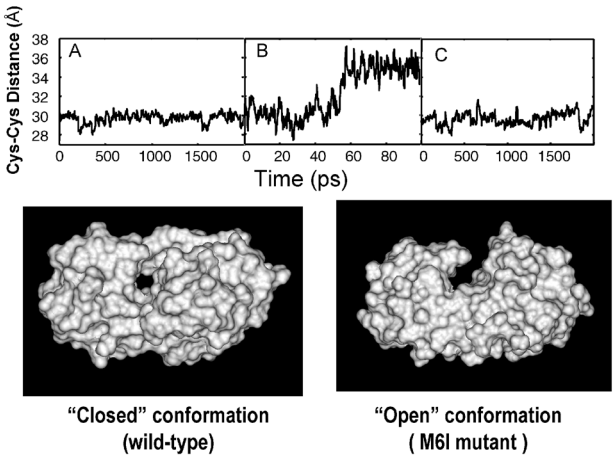

Fig. 6 Molecular dynamics simulation of T4 lysozyme hinge-bending motion. Three conformation trajectories of T4 lysozyme in solution at room temperature are presented: free enzyme without substrate (E), active enzyme-polysaccharide complex (ES*), and nonspecific binding of polysaccharide (E + S → ES). **(left panel)** The time trajectory of distance between two –SH of Cys-54 and Cys-97 of free enzyme. **(middle panel)** The time trajectory of non-active enzyme-substrate formation dynamics as the polysaccharide moves into the active site of the T4 lysozyme. **(right panel)** The time trajectory of the distance between two –SH of Cys-54 and Cys-97 of T4 lysozyme-polysaccharide active complex.[12] Enzyme structure (E) was taken from the 1.7-Å X-ray crystallographic structure (PDB entry 3LZM) and included 152 water molecules. The system was placed in a periodic cube of 73.34 Å per side and filled with 11,948 SPCE water molecules, including a section of the substrate (ES*). A six-unit oligosaccharide consisting of alternating *N*-acetylmuramic acid (NAM) and *N*-acetylglucosamine (NAG) was positioned in the active site with the aid of superimposing the lysozyme mutant adducted with substrate cleaved from the cell wall of *E. coli* (PDB entry 148L). (Bottom panel) Two conformation states of T4 lysozyme protein surface presentations based on crystal structures for wt and a mutant T4 lysozyme, showing both closed and open conformations.

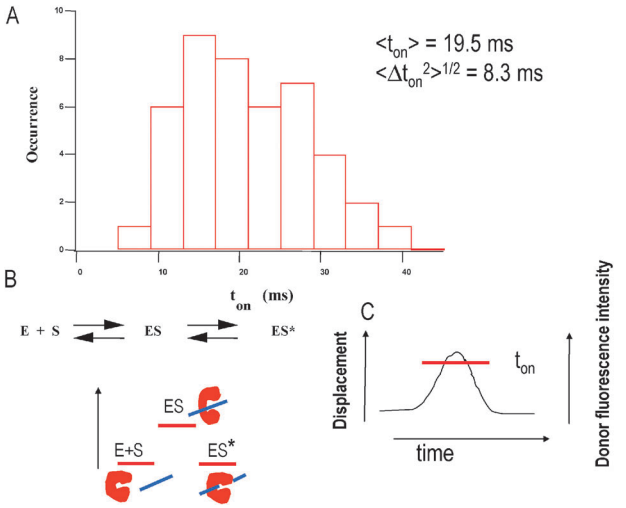

Fig. 7 (A) Active-complex, ES*, formation time (t_{open}) distribution deduced from a single T4 lysozyme fluorescence trajectory under enzymatic reaction. The t_{open} is the duration time of each wiggling of the intensity trajectory above a threshold. The threshold is determined by the 50% of the bimodal intensity distribution (see Fig. 5 inset). The mean open time, $\langle t_{open} \rangle$, is 19.5 ± 2 ms and the standard deviation of the open time is 8.3 ± 2 ms. (B) The measured t_{open} reflects the time for the formation of active enzyme-substrate complex (ES*). The enzyme active site opens up to take substrate in and form the non-specific binding complex (ES) and close down to form the active complex (ES*). The single-molecule open-close hinge-bending motions are measured by single-molecule FRET spectroscopy and recorded in the FRET time trajectories. (C) An illustration of the t_{open} measured from the donor intensity changes.

For T4 lysozyme's conformational dynamics, the physical nature of the bunching effect is associated with the functionally-conformational motion mechanism[6] involving in non-equilibrium conformational fluctuations.[16] The characteristics of the non-equilibrium conformational fluctuation dynamics is experimentally-observed by oscillatory fluctuations of the conformational open-close motions and the Gaussian-like formation time distributions.[12] The conformational dynamics is significantly regulated by the interactions between the T4 lysozyme and the substrate in terms of electrostatic attraction and hydrogen bonding interactions, being associated with the formation of the active complex state of ES* (Fig. 1 and 2) for the T4 lysozyme enzymatic reactions. Fig. 11A and B shows our simulated data for six intermediate steps using eqn (4), in which $\langle t_{open*} \rangle$ is calculated to be 19.1 ± 2 ms. Unambiguously, the simulated data shows essentially the same ES* formation time distribution with a Gaussian-like profile and the mean value of t_{open} (Fig. 11B) compared with the experimental t_{open} distribution (Fig. 11A).

Typically, functional conformation selection mechanism applies when bunching effects in the conformational dynamics existed. As a strong experimental evidence of ordered molecular conformational motions emerge from conformational fluctuations under enzymatic reaction conditions, bunching effect appeared from enzyme conformational motions has significant and general biological relevance and consequences associated with some profoundly important biological properties, including biological oscillations and self-organizations, temporal and spatial functionality and complexity, and biological rhythms.

8. Beyond the conventional correlation function analysis of complex conformational fluctuations: 2D regional correlation analysis of single-molecule time trajectories

We have developed a specific approach of 2D regional correlation analysis capable of analyzing fluctuation dynamics of complex multiple correlated and anti-correlated fluctuations under a non-correlated noise background.[57] Using this new method, we were able to map out any defined segments along a fluctuation trajectory and determine whether they are correlated, anti-correlated, or non-correlated; after which, a cross correlation analysis can be applied for each specific segment to obtain a detailed fluctuation dynamics analysis.[57]

In recent years, the extensive developments of single-molecule spectroscopy and nanotechnology have brought the fluctuation analysis as one of the mostly used analytical approaches.[3,5,8,9,10,12,35,52–58,68–73] Especially, in single molecular optical spectral analyses, correlation function is an useful

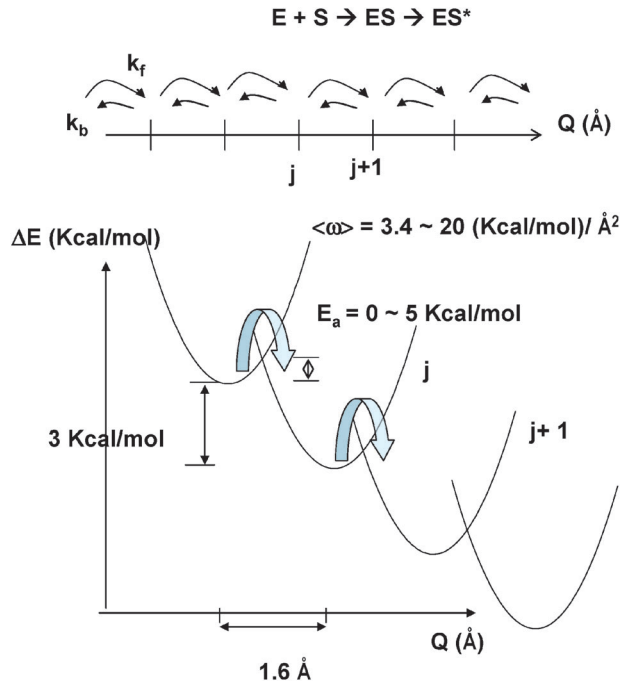

Fig. 8 Based on the results of the single-molecule spectroscopy measurements, an attempt to estimate the energy potential surface of T4 lysozyme–substrate complex formation process. The conformational change dynamics involving multiple intermediate states is analyzed based on a one-dimensional random walk model coupled with the parameters obtained from our single-molecule experimental spectroscopy and MD simulation. The conformational motion in each enzymatic turnover cycle involves six intermediate states based on the model analysis. Since the total energy change between E and ES* states is about −18 kcal mol^{-1}, assuming six intermediate states would result in an average energy difference of 3 kcal mol^{-1} for each associated conformational state along the a-helix coordinate during the hinge-bending motion. We postulate that the activation energy associated with the k_f of the forward step is about 0–5 kcal mol^{-1}, considering the slow forward rate and the entropy decrease in the complex formation process. It is reasonable to assume the energy potential surface along the conformational change nuclear coordinate to be parabolic for each intermediate state. Therefore, the averaged force constant of the potential surface for each intermediate state is calculated to be 3.4–20 kcal mol^{-1} Å^{-12}.[35]

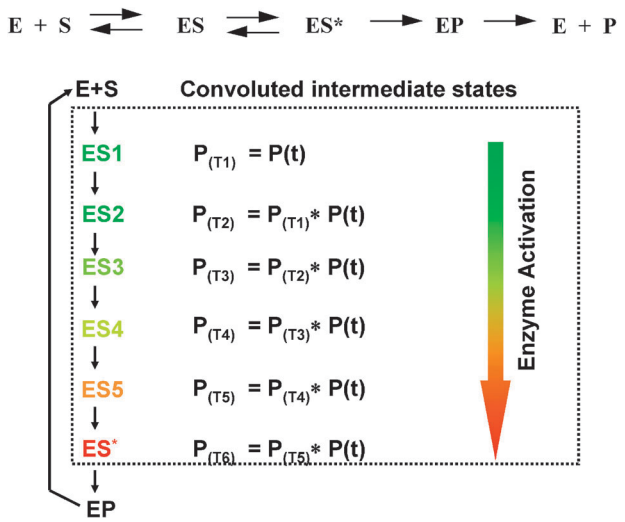

Fig. 9 A modified Mechaelis-Menton mechanism for T4 lysozyme conformational dynamics. E, S, and P represent the enzyme, substrate, and product, respectively. Scheme of the enzyme reaction and the formation-time probabilities of multiple convoluted intermediate states. From E + S to ES*, the enzyme experiences multiple intermediate states and finally reaches the active state, ES*. $P(t)$ is the probability distribution of the step times. $P_{(Tn)}$ (n = 1, 2, 3, 4, 5, 6) are the formation-time probabilities for the intermediate states, and ES* is readied for the enzymatic reaction.

method to measure molecular properties from the fluctuation time trajectories, which may contain detailed information of molecular conformational changes, reactivity, molecular interactions, and also the intrinsic and measurement noises.[3,63,74–76] However, these rather complex applications on analyzing single-molecule fluctuations have encountered some limitations for conventional correlation analyses. For example, fluctuations of molecular variables can be either correlated or anti-correlated or non-correlated depending on the nature of the variables and the temporal fluctuation of the molecular local environment.[3,5,8–10,12,35,52,58–67,77,78] A conventional correlation analysis typically calculates a correlation function based on the whole time trajectory of a physical variable. Presumably, the longer the trajectory is accounted for the calculation, the higher the signal-to-noise ratio of the analysis may have for the fluctuation dynamics. Nevertheless, this conventional approach is often incapable of revealing some critical fluctuation dynamics that intermittently appear in a complex fluctuation system under a noise background. For example, when the correlated and anti-correlated fluctuations appear intermittently in a long fluctuation time trajectory,[79] to calculate a correlation function indiscriminately accounting for the whole trajectory may detect neither of the fluctuation dynamics due to the cancellation between the correlated and anti-correlated fluctuations in such a calculation approach.

If the fluctuations are entirely originated from FRET, the fluorescence intensity fluctuations of donor and acceptor are anti-correlated due to the fact that the donor signal goes up and the acceptor signal goes down when the D–A distance increases, and the donor signal goes down and the acceptor signal goes up when the D–A distance decreases. However, under a real experimental condition, other sources of fluctuations may also exist, for example, the thermal fluctuation of the overall local environment that statistically makes both the donor and acceptor fluorescence signals go up and down together and fluctuate correlatively. Typically, measurement noise and fast fluctuation beyond the measurement time responses fluctuate non-correlatively. Often, fluctuations from different sources may dominate intermittently the overall signal fluctuation at different time segments of a fluctuation trajectory. Conventional correlation function calculation treats the whole fluctuation trajectory equally and does not identify the type changes of intermittent fluctuations, which often averages out the non-dominate types of fluctuations that can be important for understanding the complex protein conformational dynamics. We have developed a new approach of 2D regional correlation function analysis of single-molecule time trajectories to identify and differentiate the time segments

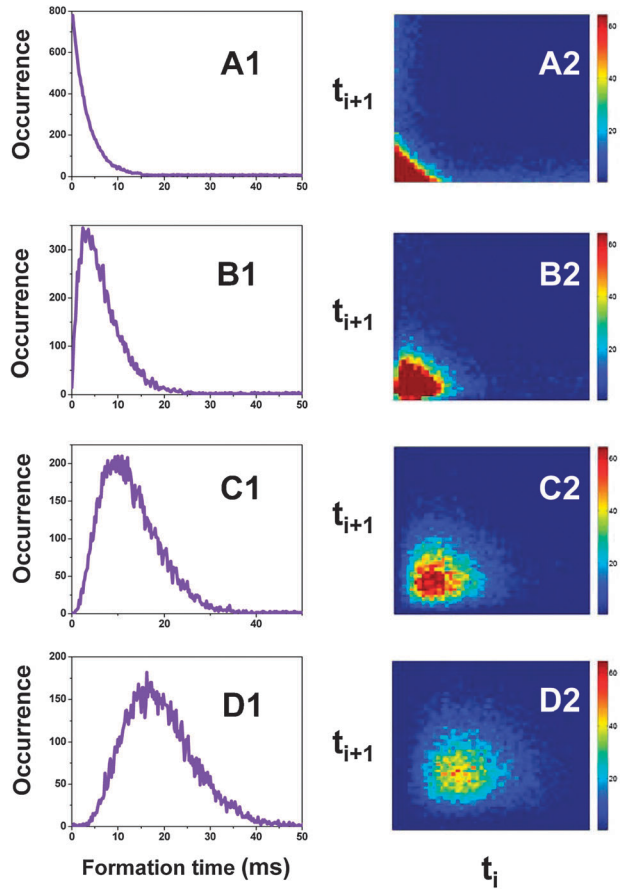

Fig. 10 Simulated distribution of formation times (A1 to D1) and corresponding two dimensional joint probability distributions (A2 to D2) of adjacent formation times for different intermediate steps. As a single step, A1 shows exponential distribution and A2 only shows a wing structure implying one step is a Poisson process and there is no bunching effect. However, for the multiple steps such as 2, 4, 6 steps, non-exponential distributions of the probabilities (in B1, C1 and D1) and the bunching structures (in B2, C2 and D2) are increasingly clear, implying the bunching nature in the open–close conformational motion times.

of correlated, anti-correlated, and non-correlated fluctuations in a long fluctuation trajectory so that the different type of fluctuations can be exclusively mapped out in a detailed analysis without averaging them out or losing the critical identification of some important fluctuation behaviors.

The cross-correlation evaluates the time-dependent strength between two fluctuating variables.[53,60–62,68] The cross-correlation ($C_{\text{cross}}(t)$) functions are defined by eqn (5) and (6).

$$\begin{aligned} C_{\text{cross}}(t) &= \langle \Delta A(0)\Delta B(t)\rangle / \langle \Delta A(0)\Delta B(0)\rangle \\ &= \langle (A(0) - \langle A\rangle)(B(t) - \langle B\rangle)\rangle / \\ &\quad \langle (A(0) - \langle A\rangle)(B(0) - \langle B\rangle)\rangle \end{aligned} \tag{5}$$

When $A = B$, we have autocorrelation function,

$$\begin{aligned} C_{\text{auto}}(t) &= \langle \Delta A(0)\Delta A(t)\rangle / \langle \Delta A(0)^2\rangle \\ &= \langle (A(0) - \langle A\rangle)(A(t) - \langle A\rangle)\rangle / \\ &\quad \langle (A(0) - \langle A\rangle)^2\rangle \end{aligned} \tag{6}$$

where $A(t)$ and $B(t)$ are the signal variables measured in time trajectories $\{A(t)\}$ and $\{B(t)\}$. $\langle A\rangle$ and $\langle B\rangle$ are the means of the fluctuation trajectories of $\{A(t)\}$ and $\{B(t)\}$, respectively. In spectroscopic fluctuation analyses, $\{A(t)\}$ and $\{B(t)\}$ can be the time trajectories of spectral intensity, spectral mean, fluorescence polarization, photon counts, and other physical parameters. Mathematically, a time-correlation function for continuous or discrete fluctuation trajectory $\{A(t)\}$ is calculated by:

$$\begin{aligned} C_{\text{auto}}(t) &= \langle \Delta A(0)\Delta A(t)\rangle / \langle \Delta A(0)^2\rangle \\ &= \int d\tau (A(\tau) - \langle A\rangle)(A(\tau - t) \\ &\quad - \langle A\rangle) / \int d\tau (A(\tau) - \langle A\rangle)^2 \end{aligned} \tag{7}$$

The cross-correlation analyses are methods to study the time-dependent behaviors of fluctuating signals.

The primary analytical approach of the 2D regional correlation analysis is to calculate a two-dimensional cross-correlation function amplitude distribution (TCAD). In this analysis, a start time and a stop time, t_{start} and t_{stop}, were scanned to chose the calculation of cross-correlation function from a two-band signal intensity time trajectory, $\{I_1(t)\}$, $\{I_2(t)\}$. The two scanning parameters, t_{start} and t_{stop}, define the start time (t_{start}) and the time lapse (from t_{start} to t_{stop}) of a cross-correlation function calculation window along a two-band fluctuation

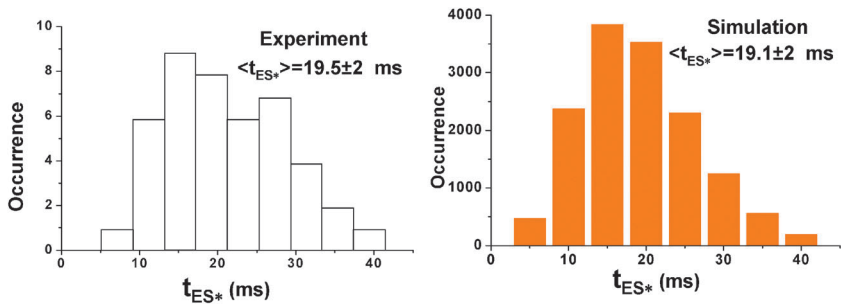

Fig. 11 Histograms of the experimental[12] and simulated formation times (t_{ES*}) of the conformational motions in forming ES*. The experimental data is deduced from a single T4 lysozyme fluorescence trajectory.[12] t_{ES*} is the duration time of each wiggling of the intensity trajectory above a threshold. The threshold is determined by 50% of the bimodal intensity distribution.[12] The mean formation times, $\langle t_{ES*}\rangle$ are 19.5 ± 2 and 19.1 ± 2 ms for the experiment and simulation, and the corresponding standard deviation of the formation time is 8.3 ± 2 and 7.5 ± 2 ms, respectively.

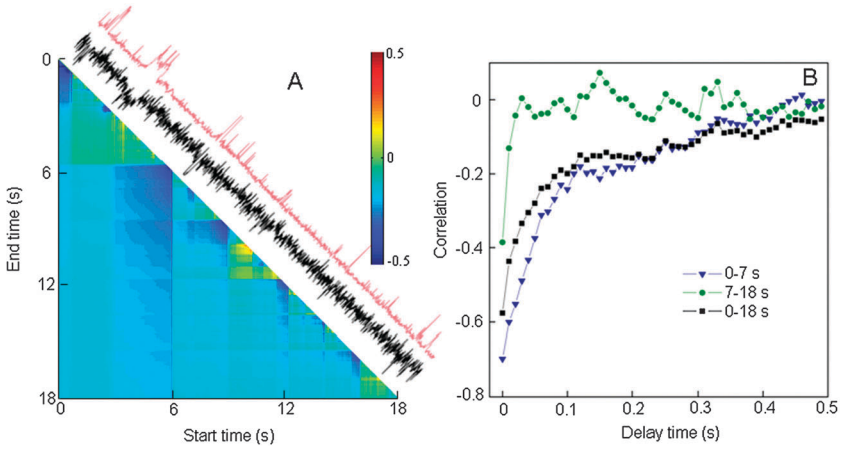

Fig. 12 An example of 2D regional correlation analysis on single-molecule FRET fluctuation data analysis. The experimental FRET two-band (D–A) fluorescence intensity fluctuation trajectory is measured from a D–A labeled kinase enzyme protein molecule involving a conformational change fluctuation in a buffer solution. (A) A TCAD map calculated from a two-band (D–A) FRET fluorescence fluctuation trajectory. The Red and black trajectories are the donor and acceptor signals, respectively. (B) Cross correlation functions calculated from different sections of the trajectory. It is clear that the dynamics can be averaged out if only a whole-trajectory calculation is obtained. The anti-correlated FRET fluctuations can only dominate the fluorescence intensity trajectories in fraction of time periods but not all the time due to non-correlated and correlated thermal fluctuation background noises.[57]

signal trajectory. This 2D calculation gives a cross-correlation for defined segments from t_{start} to t_{stop} as:

$$C_{cross}(\tau, t_{start}, : t_{stop}) = \int_{t_{start}}^{t_{stop}} I_1(t)I_2(t-\tau)\mathrm{d}t = \sum_{t_{start}}^{t_{stop}} I_1(t)I_2(t-\tau) \quad (8)$$

The window of t_{start} to t_{stop} is scanned in a range through the intensity trajectories. A cross-correlation function is calculated from a two-band fluctuation trajectory for each scanned pair of t_{start} to t_{stop}. The initial amplitude of $C(\tau, t_{start} : t_{stop})$ was presented by the difference between the first n points and the next $n+m$ points from $\tau^{\bullet} = 0$:

$$\zeta = \{\langle C(1:n)\rangle\} - \{\langle C(n+1:n+m)\rangle\} \quad (9)$$

The index n and m defines the precision of calculated initial amplitude, ζ, of the correlation function. In our analysis, we chose $n = m = 3$, which is sufficient to obtain a reliable value of ζ from the calculated cross-correlation function. As a function of t_{start} and t_{stop}, the value of ζ is plotted as a two-dimensional map of t_{start} to t_{stop}. A hot color represents positive amplitude of $C(\tau)$ and a cold color represents negative amplitude of $C(\tau)$. Positive amplitude indicates correlation, and negative amplitude indicates anti-correlation.

The significant advantage of TCAD is that both the correlated and anti-correlated spectral intensity fluctuations can be identified pixel-by-pixel for each pair of t_{start} to t_{stop} based on calculated cross correlation function pixel-by-pixel (Fig. 12). Specifically, for an analysis of the single-molecule FRET D–A two-band fluctuation trajectories, (1) the parameter of Z-axis is the amplitude of the cross correlation function from a FRET donor–acceptor two-band fluorescence intensity time trajectory. A positive amplitude means (represented by a hot color) that the two bands ($I_1(t)$ and $I_2(t)$) in an intensity trajectory fluctuate correlatively (both go up and down together) (Fig. 12A); whereas, a negative amplitude (represented by a cold color) means that the two bands ($I_1(t)$ and $I_2(t)$) in an intensity trajectory fluctuate anti-correlatively (one goes up while the other one goes down, and *vise versa*); a zero amplitude (represented by a green color) means that the two bands ($I_1(t)$ and $I_2(t)$) in an intensity trajectory fluctuate randomly without any correlation. (2) The parameters of X-Y axes represent the time window between t_{start} and t_{stop} for calculating the cross correlation functions from the FRET donor–acceptor two-band fluorescence intensity time trajectories. The t_{start} and t_{stop} of the TCAD define the time window (position and width) for the calculated cross correlation function, and the width and position of the window are scanned through the intensity trajectories by scanning all the possible values of t_{start} and t_{stop}.

The usefulness of the 2D regional correlation analysis is (1) the ability to search for the time segments when the anti-correlated FRET fluctuation is relatively larger; and then (2) specifically analyze the FRET fluctuation dynamics for that identified segment. Our analysis approach can be applied to other types of correlated or random fluctuations, including thermally-induced intensity fluctuations, fluctuation due to photobleaching of donor or acceptor probe molecules, and intensity fluctuations due to the cross-talking in detecting the donor–acceptor two-band intensity trajectories.

9. Concluding remarks and future perspectives

In biological systems, enzymatic reactions typically involve multiple kinetic steps, complex molecular interactions, complex conformational changes, and confined local environments. These complexities, associated with intrinsic spatial and temporal inhomogeneities, often make a solution-phase ensemble-averaged measurement inadequate. In many systems, only the overall enzymatic reaction rates are measured without further characterization of kinetic mechanism, intermediate states, and step-specific reaction rates. Single-molecule spectroscopy, studying

one molecule under a specific physiological condition at a time, is potentially a powerful and unique approach to characterize and analyze the complex enzymatic reaction dynamics and the correlated conformational change dynamics. An even more informative and powerful methodology is to combine single-molecule spectroscopy, computational molecular dynamics, and theoretical modeling, an approach that provides molecular-level characterization of the enzymatic reaction dynamics, conformational dynamics, and energy landscape of specific conformational changes. It is the active complex formation processes ($E + S \rightarrow ES \rightarrow ES^*$) that define the enzymatic reaction potential surfaces and contribute to the complexity and inhomogeneity of the enzymatic reactions. Understanding enzymatic reaction conformational dynamics is intimately related to single-molecule studies of biomolecular interactions for the precise reason that the formation of an enzymatic reaction active complex involves biomolecular interactions. In recent years, mechanisms of protein conformation selection and induced conformational changes have been extensively explored,[92–103] and it is anticipated that more single-molecule protein-protein interaction studies will also contribute to our fundamental understanding of enzymatic reaction dynamics and mechanisms. One of the most exciting research fields is multiple probe FRET to simultaneously probing multiple coordinates of the enzyme conformational change dynamics to evaluate possible cooperativity and allosteric dynamics.[107–109] Applying the combined approaches, we have begun to obtain detailed mechanistic information about enzymatic conformational dynamics, including the intermediate enzyme-substrate complex structures and the associated energy landscape.[35] Correlated mechanical force pulling to perturb enzyme conformational dynamics and reactivity is another new research field that holds high promise of manipulate and regulate enzyme activities in order to explore new enzyme properties and obtain fundamental understanding of enzymatic dynamics.[95–97] The next generation of single-molecule spectroscopy will be not only capable of probing complex single-molecule protein dynamics but also capable of manipulating protein conformational dynamics and control protein activities. The new single-molecule spectroscopy will be powerful in exploring unprecedented protein properties, protein dynamics, and protein function energetic landscapes.

Acknowledgements

The author thanks Dehong Hu, Yuanmin Wang, Xuefei Wang, Yu Chen, and Erich R. Vorpagel, for their crucial contributions to the work discussed here; Brian Matthews for providing us with T4 lysozyme proteins, and the recipe for preparing the substrate. We also acknowledge the support to our program from the Chemical Sciences Division of the Office of Basic Energy Sciences (BES) within the Office of Energy Research of the U.S. Department of Energy (DOE), The US Defense Advanced Research Projects Agency (DARPA), the Material Science Division of the US Army Research Office (ARO), National Science Foundation (NSF), National Institute of Environmental Health Sciences (NIEHS) of National Institute of Health (NIH), National Institute of Gerneral Medicine Sciences (NIGMS) of NIH, Bowling Green State University, Pacific Northwest National Laboratory, and Ohio Eminent Scholar Endowment. Part of the text appeared in our previous publications referenced.

References

1 Q. Xue and E. S. Yeung, Differences in the chemical reactivity of individual molecules of an enzyme, *Nature*, 1995, **373**, 681.
2 D. G. Craig, E. A. Arriaga, J. C. Y. Wong, H. Lu and N. J. Dovichi, Studies on single alkaline phosphatase molecules: reaction rate and activation energy of a reaction catalyzed by a single molecule and the effect of thermal denaturation-the denaturation of an enzyme, *J. Am. Chem. Soc.*, 1996, **118**, 5245.
3 H. P. Lu, L. Xun and X. S. Xie, Single-molecule enzymatic dynamics, *Science*, 1998, **282**, 1877; X. S. Xie and H. P. Lu, *J. Biol. Chem.*, 1999, **274**, 15967.
4 B. English, W. Min, A. van Oijen, K. Lee, G. Luo, H. Sun, B. Cherayil, S. Kou and X. S. Xie, *Nat. Chem. Biol.*, 2006, **2**, 87–94.
5 L. Edman and R. Rigler, *Proc. Natl. Acad. Sci. U. S. A.*, 2000, **97**, 8266; H. Lerch, R. Rigler and A. Mikhailov, *Proc. Natl. Acad. Sci. U. S. A.*, 2005, **102**, 10807.
6 R. Zwanzig, *Acc. Chem. Res.*, 1990, **23**, 148.
7 J. Wang and P. Wolynes, *Phys. Rev. Lett.*, 1995, **74**, 4317.
8 G. K. Schenter, H. P. Lu and X. S. Xie, *J. Phys. Chem. A*, 1999, **103**, 10477.
9 N. Agmon, *J. Phys. Chem. B*, 2000, **104**, 7830.
10 H. P. Lu, L. M. Iakoucheva and E. J. Ackerman, *J. Am. Chem. Soc.*, 2001, **123**, 9184; H. P. Lu, L. M. Iakoucheva and E. J. Ackerman, Single-molecule DNA damage recognition: DNA-protein and protein-protein interaction dynamics, *Biophys. J.*, 2000, **78**, 262A.
11 A. M. van Oijen, P. C. Blainey, D. J. Crampton, C. C. Richardson, T. Ellenberger and X. S. Xie, *Science*, 2003, **301**, 1235.
12 Y. Chen, D. Hu, E. R. Vorpagel and H. P. Lu, *J. Phys. Chem. B*, 2003, **107**, 7947.
13 Part of the text appeared in a review article, *Curr. Pharm. Biotech.*, 2004, **5**, p. 261.
14 B. W. Matthews, *Adv. Protein Chem.*, 1995, **46**, 249.
15 X. J. Zhang, J. A. Wozniak and B. W. Matthews, *J. Mol. Biol.*, 1995, **250**, 527.
16 H. R. Faber and B. W. Matthews, *Nature*, 1990, **348**, 263.
17 R. Kuroki, L. H. Weaver and B. W. Matthews, *Science*, 1993, **262**, 2030.
18 G. E. Arnold and R. L. Ornstein, *Biopolymers*, 1997, **41**, 533.
19 L. Edman, Z. Foldes-Papp, S. Wennmalm and R. Rigler, The fluctuating enzyme: a single molecule approach, *Chem. Phys.*, 1999, **247**, 11.
20 L. Edman and R. Rigler, Memory landscapes of single-enzyme molecules, *Proc. Natl. Acad. Sci. U. S. A.*, 2000, **97**, 8266.
21 R. Polakowski, D. B. Craig, A. Skelley and N. J. Dovichi, Single Molecules of Highly Purified Bacterial Alkaline Phosphatase Have Identical Activity, *J. Am. Chem. Soc.*, 2000, **122**, 4853.
22 B. W. Matthews, Studies On Protein Stability With T4 Lysozyme, *Adv. Protein Chem.*, 1995, **46**, 249.
23 X. J. Zhang, J. A. Wozniak and B. W. Matthews, Protein Flexibility And Adaptability Seen In 25 Crystal Forms Of T4 Lysozyme, *Philips Res. Rep.*, 1995, **250**, 527.
24 H. R. Faber and B. W. Matthews, A Mutant T4 Lysozyme Displays 5 Different Crystal Conformations, *Nature*, 1990, **348**, 263.
25 R. Kuroki, L. H. Weaver and B. W. Matthews, A covalent enzyme-substrate intermediate with saccharide distortion in a mutant T4 lysozyme, *Science*, 1993, **262**, 2030.
26 H. S. Mchaourab, K. J. Oh, C. J. Fang and W. L. Hubbell, Conformation of T4 Lysozyme in Solution. Hinge-Bending Motion and the Substrate-Induced Conformational Transition Studied by Site-Directed Spin Labeling, *Biochemistry*, 1997, **36**, 307.
27 G. Wagner, S. G. Hyberts and T. F. Havel, NMR Structure Determination in Solution: A Critique and Comparison with

X-Ray Crystallography, *Annu. Rev. Biophys. Biomol. Struct.*, 1992, **21**, 167.
28 E. J. Hustedt and A. H. Beth, Nitroxide Spin–Spin Interactions: Applications to Protein Structure and Dynamics, *Annu. Rev. Biophys. Biomol. Struct.*, 1999, **28**, 129.
29 S. Hayward and H. J. C. Berendsen, Systematic Analysis of Domain Motions in Proteins from Conformations Change: New Results on Citrate Synthase and T4 Lysozyme, *Proteins: Struct., Funct., Bioinf.*, 1998, **30**, 144.
30 G. E. Arnold and R. L. Ornstein, Protein Hinge bending as seen in molecular dynamics simulations of native and M6I mutant T4 lysozymes, *Biopolymers*, 1997, **41**, 533.
31 H. P. Lu and X. S. Xie, Single-molecule spectral fluctuations at room temperature, *Nature*, 1997, **385**, 143.
32 X. S. Xie and H. P. Lu, Single-molecule enzymology, *J. Biol. Chem.*, 1999, **274**, 15967; G. K. Schenter, H. P. Lu and X. S. Xie, Statistical analyses and theoretical models of single-molecule enzymatic dynamics, *J. Phys. Chem. A*, 1999, **103**, 10477.
33 S. Weiss, *Science*, 1999, **283**, 1676.
34 A. Tsugita, M. Inouye, E. Terzaghi and G. Streisinger, *J. Biol. Chem.*, 1968, **243**, 391.
35 H. P. Lu, *Acc. Chem. Res.*, 2005, **38**, 557–565.
36 H. Peter Lu, Acquiring a Nano-View of Single Molecules in Actions, *Nano Rev.*, 2010, **1**, 6–7.
37 I. Oppenheim, K. E. Shuler and G. H. Weiss, *Stochastic Processes in Chemical Physics: The Master Equation*, The MIT Press, Cambridge, MA, 1977.
38 M. Vergeles and G. Szamel, *J. Chem. Phys.*, 1999, **110**, 6827.
39 J. E. Straub, M. Brokovec and B. J. Berne, *J. Phys. Chem.*, 1987, **91**, 4995.
40 D. Chandler, *Introduction to Modern Statistical Mechanics*, Oxford university Press, Oxford, 1987.
41 Dehong Hu and H. Peter Lu, Single-Molecule Nanosecond Anisotropy Dynamics of Tethered Protein Motions, *J. Phys. Chem. B*, 2003, **107**, 618.
42 Yuanmin Wang and H. Peter Lu, Bunching Effect in Single-Molecule T4 Lysozyme Non-Equilibrium Conformational Dynamics under Enzymatic Reactions, *J. Phys. Chem. B*, 2010, **114**, 6669–6674.
43 P. G. Wolynes, *Philos. Trans. R. Soc. London, Ser. A*, 2005, **363**, 453–467.
44 H. P. Lerch, R. Rigler and A. S. Mikhailov, *Proc. Natl. Acad. Sci. U. S. A.*, 2005, **102**, 10807–10812.
45 W. J. Greenleaf, M. T. Woodside and S. M. Block, *Annu. Rev. Biophys. Biomol. Struct.*, 2007, **36**, 171–190.
46 Q. Lu and J. Wang, *J. Am. Chem. Soc.*, 2008, **130**, 4772–4783.
47 M. O. Vlad, F. Moran, F. W. Schneider and J. Ross, *Proc. Natl. Acad. Sci. U. S. A.*, 2002, **99**, 12548–12555.
48 E. Tan, T. J. Wilson, M. K. Nahas, R. M. Clegg, D. M. J. Lilley and T. Ha, *Proc. Natl. Acad. Sci. U. S. A.*, 2003, **100**, 9308–9313.
49 J. Zhang, C. J. Lu, K. Chen, W. L. Zhu, X. Shen and H. L. Jiang, *Proc. Natl. Acad. Sci. U. S. A.*, 2006, **103**, 13368–13373.
50 O. A. Sytina, D. J. Heyes, C. N. Hunter, M. T. Alexandre, I. H. M. van Stokkum, R. van Grondelle and M. L. Groot, *Nature*, 2008, **456**, 1001–1004.
51 S. D. Lahiri, G. Zhang, D. Dunaway-Mariano and K. N. Allen, *Science*, 2003, **299**, 2067–2071.
52 S. Yang and J. Cao, *J. Chem. Phys.*, 2002, **117**, 10996–11009.
53 L. Edman and R. Rigler, *Proc. Natl. Acad. Sci. U. S. A.*, 2000, **97**, 8266–8271.
54 X. Zhuang, H. Kim, M. J. B. Pereira, H. P. Babcock, N. G. Walter and S. Chu, *Science*, 2002, **296**, 1473–1476.
55 I. Oppenheim, K. E. Shuler and G. H. Weiss, *Stochastic processes in chemical physics: the master equation*, The MIT Press, Cambridge, MA, 1977.
56 R. Zwanzig, *Nonequilibrium statistical mechanics*, Oxford University Press, USA, 2001.
57 Xuefei Wang and H. Peter Lu, 2D Regional Correlation Analysis of Single-Molecule Time Trajectories, *J. Phys. Chem. B*, 2008, **112**, 14920–14926.
58 E. Barkai, Y. Jung and R. Silbey, *Phys. Rev. Lett.*, 2001, **87**, 207403-1.
59 R. M. Dickson, A. B. Cubitt, R. Y. Tsien and W. E. Moerner, *Nature*, 1997, **388**, 355.
60 L. Edman, Z. Foldes-Papp, S. Wennmalm and R. Rigler, *Chem. Phys.*, 1999, **247**, 11.
61 L. Edman, U. Mets and R. Rigler, *Proc. Natl. Acad. Sci. U. S. A.*, 1996, **93**, 6710.
62 Y. W. Jia, D. S. Talaga, W. L. Lau, H. S. M. Lu, W. F. DeGrado and R. M. Hochstrasser, *Chem. Phys.*, 1999, **247**, 69.
63 H. P. Lu and X. S. Xie, *Nature*, 1997, **385**, 143.
64 S. Maiti, U. Haupts and W. W. Webb, *Proc. Natl. Acad. Sci. U. S. A.*, 1997, **94**, 11753.
65 N. G. V. Kamper and I. Oppenheim, *Stochastic processes in physics and chemistry*, 1992, 335.
66 J. Wang and P. Wolynes, *Phys. Rev. Lett.*, 1995, **74**, 4317.
67 J. Wang and P. Wolynes, *J. Chem. Phys.*, 1999, **110**, 4812.
68 H. P. Lu and X. S. Xie, *J. Phys. Chem. B*, 1997, **101**, 2753.
69 M. Lippitz, F. Kulzer and M. Orrit, *ChemPhysChem*, 2005, **6**, 770.
70 D. A. Mcquarrie, *Statistical Mechaniscs*, HARPER & ROW, New York, 1973.
71 L. Edman, *J. Phys. Chem. A*, 2000, **104**, 6165.
72 R. Rigler and H. Vogel, *Single Molecules and Manotechnology*, Springer, 2008.
73 R. Erdmann, J. Enderlein and C. Seidel, *Cytometry*, 1999, **36**, 162.
74 B. Sakmann and E. Neher, *Single Channel Recordings*, 2nd ed., Kluwer, New York, 2001.
75 I. Oppenheim, K. E. Shuler and G. H. Weiss, *Stochastic processes in physics and chemistry*, the MIT press, Cambridge, 1977.
76 D. A. Bussian, M. A. Summers, B. Liu, G. C. Bazan and S. K. Buratto, *Chem. Phys. Lett.*, 2004, **388**, 181.
77 C. Buranachai, S. A. McKinney and T. Ha, *Nano Lett.*, 2006, **6**, 496.
78 J. Shi, A. Gafni and D. Steel, *Eur. Biophys. J. with Biophys. Lett.*, 2006, **35**, 633.
79 D. Pan, D. H. Hu, R. C. Liu, X. H. Zeng, S. Kaplan and H. P. Lu, *J. Phys. Chem. C*, 2007, **111**, 8948.
80 (*a*) A. Ishijima, H. Kojima, T. Funatsu, M. Tokunaga, H. Higuchi, H. Tanaka and T. Yanagida, *Cell*, 1998, **92**, 161; (*b*) H. Noji, R. Yasuda, M. Yoshida and K. Kinosita, *Nature*, 1997, **386**, 299.
81 T. J. Ha, A. Y. Ting, J. Liang, W. B. Caldwell, A. A. Deniz, D. S. Chemla, P. G. Schultz and S. Weiss, *Proc. Natl. Acad. Sci. U. S. A.*, 1999, **96**, 893.
82 M. Bates, B. Huang, G. T. Dempsey and X. W. Zhuang, *Science*, 2007, **317**, 1749.
83 S. Hohng, C. Joo and T. Ha, *Biophys. J.*, 2004, **87**, 1328.
84 N. K. Lee, *et al.*, *Biophys. J.*, 2007, **92**, 303.
85 M. Bohmer, F. Pampaloni, M. Wahl, H. Rahn, R. Erdmann and J. Enderlein, *Rev. Sci. Instrum.*, 2001, **72**, 4145.
86 J. R. Fries, L. Brand, C. Eggeling, M. Kollner and C. A. M. Seidel, *J. Phys. Chem.*, 1998, **102**, 6601.
87 J. N. Forkey, M. E. Quinlan and Y. E. Goldman, *Prog. Biophys. Mol. Biol.*, 2000, **74**, 1.
88 E. J. G. Peterman, H. Sosa, L. S. B. Goldstein and W. E. Moerner, *Biophys. J.*, 2001, **81**, 2851.
89 R. Y. Tsien and A. Miyawaki, *Science*, 1998, **280**, 1954; R. Y. Tsien, *Annu. Rev. Biochem.*, 1998, **67**, 509.
90 R. Liu, D. Hu, X. Tan and H. P. Lu, *J. Am. Chem. Soc.*, 2006, **128**, 10034.
91 X. Tan, D. Hu, T. C. Squier and H. P. Lu, *Appl. Phys. Lett.*, 2004, **85**, 2420.
92 B. Ma, S. Kumar, C. J. Tsai and R. Nussinov, *Protein Eng., Des. Sel.*, 1999, **12**, 713; O. F. Lange, *et al.*, *Science*, 2008, **320**, 1471.
93 D. E. Koshland, *Proc. Natl. Acad. Sci. U. S. A.*, 1958, **44**, 98.
94 R. Grunberg, J. Leckner and M. Nilges, *Structure*, 2004, **12**, 2125.
95 Yufan He, Xiaohua Zeng, Saptarshi Mukherjee, Suneth Rajapaksha, Samuel Kaplan and H. Peter Lu, Revealing Linear Aggregates of Light Harvesting Antenna Proteins in Photosynthetic Membranes, *Langmuir*, 2010, **26**, 307–313; V. Biju, D. Pan, Yuri A. Gorby, Jim Fredrickson, J. Mclean, D. Saffarini and H. Peter Lu, Correlated Spectroscopic and Topographic Characterization of Nanoscale Domains and Their Distributions of a Redox Protein on Bacterial Cell Surfaces, *Langmuir*, 2007, **23**, 1333–1338; Duohai Pan, Nick Klymyshyn, Dehong Hu and Peter Lu, Tip-enhanced near-field Raman spectroscopy probing single dye-sensitizedTiO2 nanoparticles, *Appl. Phys. Lett.*, 2006, **88**, 093121.

96 E. M. Puchner and H. E. Gaub, *Exploring the Conformation-Regulated Function of Titin Kinase by Mechanical Pump and Probe Experiments with Single Molecules*, Angewandte Chemie-International Edition, 2010, vol. **49**(6), pp. 1147–1150; H. Gumpp, S. W. Stahl, M. Strackharn, E. M. Puchner and H. E. Gaub, *Ultrastable combined atomic force and total internal fluorescence microscope*, Review of Scientific Instruments, 2009, vol. **80**(6).
97 S. K. Kufer, M. Strackharn, S. W. Stahl, H. Gumpp, E. M. Puchner and H. E. Gaub, *Optically monitoring the mechanical assembly of single molecules*, Nature Nanotechnology, 2009, vol. **4**(1), pp. 45–49.
98 Kerstin Blank, Gert De Cremer and Johan Hofkens, Fluorescence-based analysis of enzymes at the single-molecule level, *Biotechnol. J.*, 2009, **4**, 465–479.
99 R. Derike Smiley and Gordon G. Hammes, Single Molecule Studies of Enzyme Mechanisms, *Chem. Rev.*, 2006, **106**(8), 3080–3094.
100 Kelly Velonia *et al.*, *Single-Enzyme Kinetics of CALB-Catalyzed Hydrolysis*, Angewandte Chemie-International Edition, 2005, vol. **44**(4), pp. 560–564.
101 *Single Molecule Dynamics in Life Science*, Toshio Yanagida and Yoshiharu Ishii, ed. Wiley-VCH, Weinheim, 2009.
102 *Single Molecules and Nanotechnology*, R. Rigler and H. Vogel, ed. Springer, Berlin, 2008.
103 *Theory and Evaluation of Single-Molecule Sigbals*, Eli Barkai, Frank Brown, Michel Orrit and Haw Yang, ed. World Scientific, New Jersey, 2008.
104 Michael A. Lomholt, Michael Urbakh, Ralf Metzler and Joseph Klafter, Manipulating Single Enzymes by an External Harmonic Force, *Phys. Rev. Lett.*, 2007, **98**, 168302.
105 Yannick Rondelez, Guillaume Tresset, Kazuhito V. Tabata, Hideyuki Arata, Hiroyuki Fujita, Shoji Takeuchi and Hiroyuki Noji, Microfabricated arrays of femtoliter chambers allow single molecule enzymology, *Nat. Biotechnol.*, 2005, **23**, 361–365.
106 Hans H. Gorris and David R. Walt, Mechanistic Aspects of Horseradish Peroxidase Elucidated through Single-Molecule Studies, *J. Am. Chem. Soc.*, 2009, **131**, 6277–6282.
107 S. Hohng, C. Joo and T. Ha, Single-molecule three-color FRET, *Biophys. J.*, 2004, **87**, 1328–1337.
108 N. K. Lee, *et al.* Three-color alternating-laser excitation of single molecules: Monitoring multiple interactions and distances, *Biophys. J.*, 2007, **92**, 303–312.
109 M. Bates, B. Huang, G. T. Dempsey and X. W. Zhuang, Multi-color super-resolution imaging with photo-switchable fluorescent probes, *Science*, 2007, **317**, 1749–1753.
110 A Themed Issue on Single Molecule Spectroscopy,, *Physical Chemistry Chemical Physics*,**5**, 1697–1900.